Section 1
LASER SYSTEM REPORT

1.A GDL Facility Report

During the first quarter of FY85, the upgrade of the glass development laser (GDL) facility was started and completed. This includes successful installation and activation of active mirror amplifiers. Limited damage test experiments and target interaction experiments in the Beta target chamber were also conducted. A detailed description of the active mirror amplifiers is given in Section 1.C.

The frequency conversion cells were assembled and will be installed soon. A multi-wavelength energy-sensing system (MESS) similar to the OMEGA system has been designed, and appropriate software for acquisition and reduction of beamline energy data has been implemented. This will all be installed in the GDL system during the next shutdown period, after 1 January 1985.

During this quarter, the GDL facility was used as a single-beam IR laser with substantially more energy output.

A summary of GDL operations during this quarter follows:

Interaction Shots		73
Damage-Testing Shots		134
Alignment, Test Shots		163
	TOTAL	370

ACKNOWLEDGMENT

This work was supported by the U.S. Department of Energy Office of Inertial Fusion under agreement number DE-FC08-85DP40200 and by the Laser Fusion Feasibility Project at the Laboratory for Laser Energetics which has the following sponsors: Empire State Electric Energy Research Corporation, General Electric Company, New York State Energy Research and Development Authority, Northeast Utilities Service Company, Ontario Hydro, Southern California Edison Company, The Standard Oil Company, and University of Rochester. Such support does not imply endorsement of the content by any of the above parties.

1.B OMEGA Facility Report

OMEGA operations for this quarter consisted of work in the following areas: (a) completion of the wavelength conversion of the second group of six OMEGA beams from an IR (1054-nm) to a UV (351-nm) output; (b) activation of the 12 frequency-tripled beams; (c) target irradiation experiments with these 12 beams; and (d) cessation of laser operation for the final frequency conversion of the remaining 12 beams.

During October the components were assembled and installed for the conversion, and the first successful 12-beam target shot was achieved. The 12-beam system was fully characterized, and included a full scan of the beam waists of the focused beams, near-field photographs of all 12 beams, and a fine tuning of all conversion cells. Modifications to the polarization in the driver improved its output energy, allowing beamline energy to exceed 1 kJ; the highest energy achieved was 1056 J.

During this period, several new diagnostic instruments were activated. In particular, the radiation chemistry system has been successfully implemented, activated, and tested. The initial results were good. During the x-ray laser experiments, the activation of the shuttle target positioner allowed targets to be inserted into the target chamber without the need for a vacuum break. At the beginning of the x-ray laser campaign, cylindrical correction lenses were installed into the focus lens mounts, allowing line-focused beams to be put onto targets. Alignment techniques were devised to allow these line beams to be targeted in different configurations on both planar and cylindrical targets.

Laser operations ceased in November in order to enable frequency conversion of the last 12 beams of OMEGA. Prior to the cessation, the MESS photodiodes were precalibrated. In the calibration, the active 12 beams were used as energy sources and the calibrated diodes in the integrating spheres as the references. By this precalibration, much time can be saved during the 24-beam activation, obviating the calibration of the new photodiodes. During the last part of November and the early part of December, structures for the last 12 beams were placed and alignment of the beamlines was completed. Other activities for the 24-beam conversion during this quarter included: (a) construction, sizing, and alignment of spatial filters; (b) modification to the driver line, allowing higher output energy; (c) an attempt to eliminate the spark-gap firing of Pockels cells 4 and 5; and (d) an upgrade of the beam diagnostics package in the driver. As a result, completion of the 24-beam OMEGA UV-laser system is on schedule.

A summary of OMEGA operations during this quarter follows:

Software Test Shots		21
Driver Test Shots		75
Beamline Test Shots		50
Target Shots		88
	TOTAL	234

ACKNOWLEDGMENT

This work was supported by the U.S. Department of Energy Office of Inertial Fusion under agreement number DE-FC08-85DP40200 and by the Laser Fusion Feasibility Project at the Laboratory for Laser Energetics which has the following sponsors: Empire State Electric Energy Research Corporation, General Electric Company, New York State Energy Research and Development Authority, Northeast Utilities Service Company, Ontario Hydro, Southern California Edison Company, The Standard Oil Company, and University of Rochester. Such support does not imply endorsement of the content by any of the above parties.

1.C GDL Facility Upgrade

LLE has been engaged in the development of various Nd:glass amplifiers over the past ten years.[1,2] Development of the active mirror amplifier did not progress significantly until midway in this ten-year period, when in-house thin-film design and fabrication were made available. Concurrent with major advancements in hardware development, this thin-film capability contributed to the successful implementation of a four-unit, 17-cm clear aperture active mirror system.[3] Soon afterwards, preliminary studies of a 25-cm active mirror prototype revealed several unanticipated problems with the mounting, sealing, and coolant flow designs that were not encountered on the smaller version of the active mirror amplifier.

Recent progress in hardware development involving a new active mirror mounting and sealing design has resulted in the successful upgrade of GDL with four 25-cm-diameter active mirror amplifiers. The key features of the active mirror design are illustrated in Fig. 21.1. A 3-cm-thick LHG-8 slab is situated within an annulus of parasitic-inhibiting glass beads and is held firm with a conventional three-point mounting scheme. A bead of silicon-based sealant attaches the edge of the slab to the mirror holder, thus forming the front half of a liquid tight seal. This technique reduces the problem of pressure-induced slab distortions, previously caused by O-ring seals, without compromising the reliability of the liquid seal. The cooling system is also designed to minimize slab distortions. A mixture of ethylene glycol and water is pumped from an external reservoir to the top of the channel between the blast shield and the rear surface of the slab; at the same time, the coolant leaves the bottom of the channel to bring the mirror and the reservoir in gravitational equilibrium. This flow provides adequate cooling without significant slab distortion.

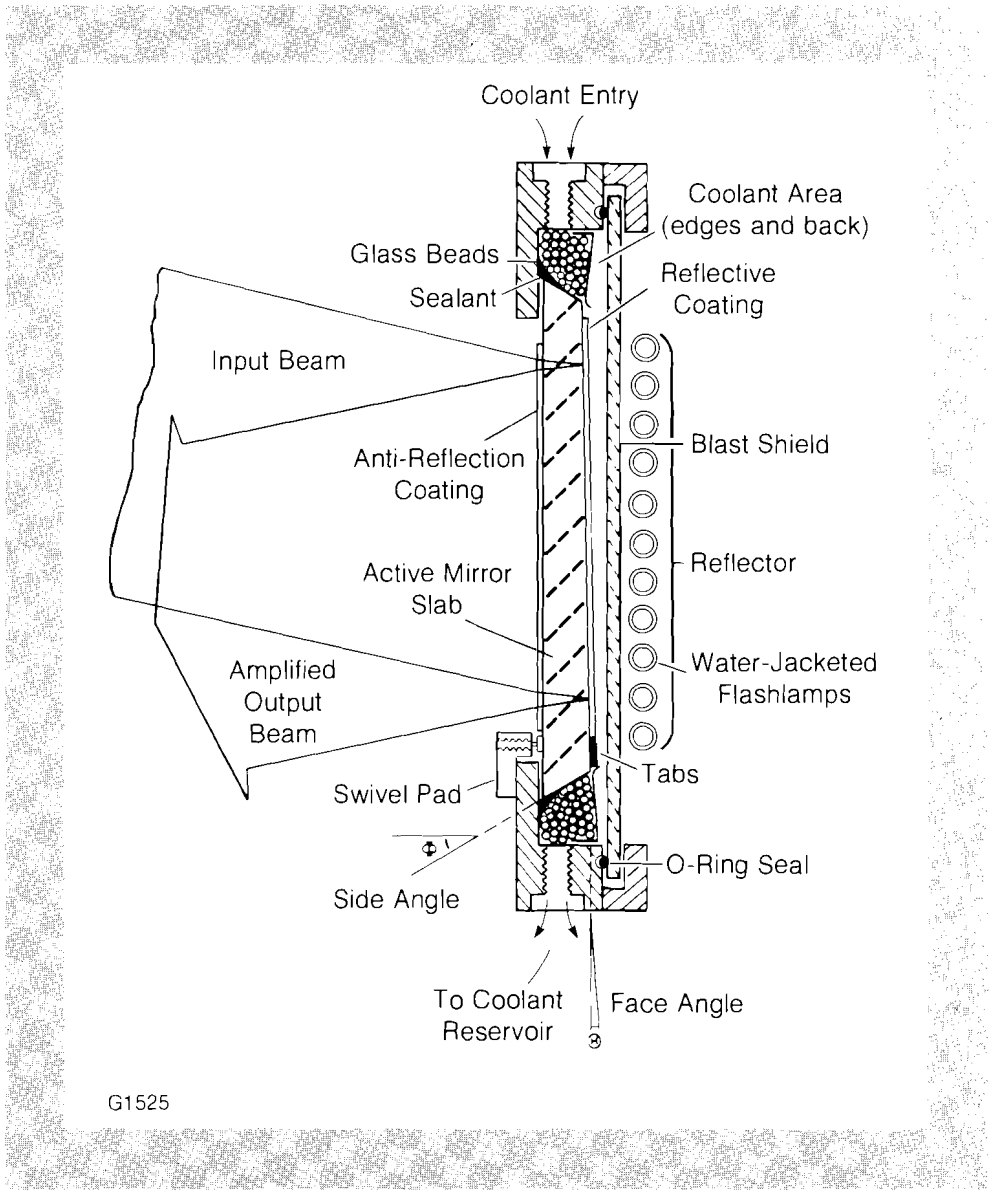

Fig. 21.1
Key features of the active mirror design. The slab is pumped by flash-lamp light entering through the surface facing the blast shield. This surface is coated to transmit useful pump bands and reflects the laser beam to be amplified. The incident laser beam enters through the front of the slab, reflects from the rear surface and exits, completing an energy-extraction path that is twice the slab thickness.

The optical pump module contains an array of water-jacketed xenon flash lamps which are closely coupled to the mirror holder. The flash lamps vary in length in order to form three pulse-forming networks of equal, total discharge length. The active mirror slab is pumped by the flash-lamp light entering through the surface facing the array. This surface is coated to allow useful pump bands to be transmitted into the slab while reflecting the laser light to be amplified. The laser beam thus makes a double pass through the slab and completes an energy extraction path that is twice the slab thickness.

During the active mirror upgrade to GDL, many improvements were made from both an operational and an experimental point of view. The laser system is schematically illustrated in Fig. 21.2. The Faraday rotator is repositioned between the second 64-mm and the 90-mm rod amplifiers to provide optical isolation between two major gain sections of the laser system. Liquid crystal circular polarizers are located throughout the

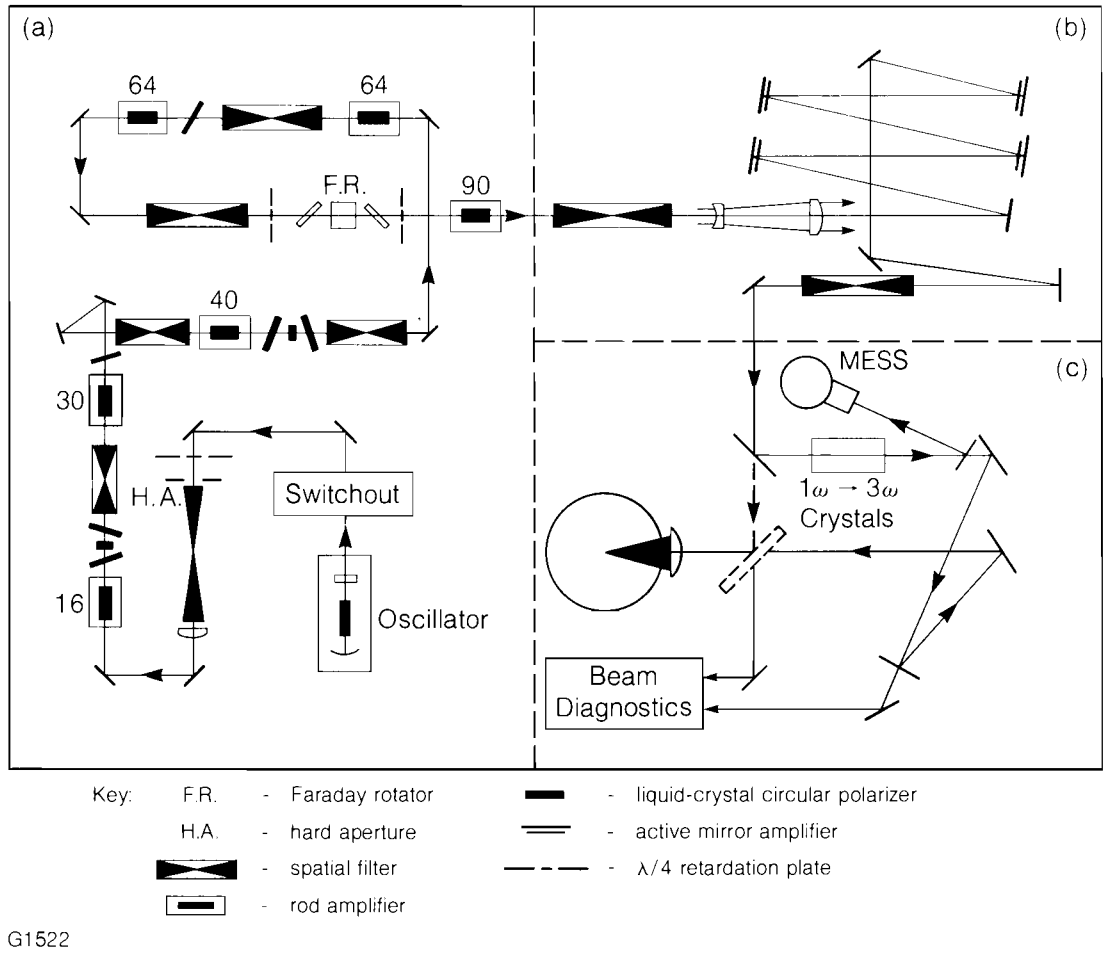

Fig. 21.2
The GDL system (a) characterized by six amplification stages that follow an active/passive mode-locked oscillator, operating at 1054 nm in 1-ns pulses. The output is upcollimated to 20-cm diameter and directed to a series of four active mirror amplifiers (b). The amplified IR beam either propagates directly into the Beta target chamber for 1-μm experiments or is frequency converted for short-wavelength experiments (c).

driver line to allow for the propagation of circularly polarized light through each of the rod amplifiers. The main advantages of this polarization scheme are described in Section 1.D.

The output of the previous GDL system is upcollimated to a beam diameter of 20 cm and directed into a series of four active mirror amplifiers. Figure 21.2(b) schematically illustrates the single-pass configuration, where the incident laser beam reflects only once from each of the active mirrors. Alternatively, in the double-pass option,[4] a retroreflecting mirror is positioned after the fourth active mirror in order to return the laser beam through the same series of active mirrors. In this scheme, a thin-film polarizer and mica quarter-wave plate are employed to separate the forward and return beams. In either configuration, the laser beam leaving the active mirror amplifiers is spatially filtered and injected into the Beta irradiation facility. Then the IR beam either propagates directly into the target chamber for IR interaction experiments or is frequency converted for short-wavelength interaction experiments [see Fig. 21.2(c)].

The active mirror single-pass and double-pass performances at 1 ns have been studied in detail. The overall active mirror gain, shown in Fig. 21.3, represents the case where only one of the four single-passed slabs has a front face coating. Although the total output was thus reduced by multiple Fresnel reflection losses, the active mirror amplifiers have produced in excess of 300 J at 1054 nm in 1-ns pulses. Unfortunately, the double-pass performance is not only reduced by the multiple Fresnel losses but also suffers from stored energy depletion due to the numerous Fresnel-reflection-generated beams which are separated slowly from the main laser beam. Additionally, a 27% loss is suffered from the polarization components required to separate the forward and returning laser beams. However, it is expected that the double-pass gain will be significantly increased once the front surface of each of the four active mirrors is AR coated in the near future.

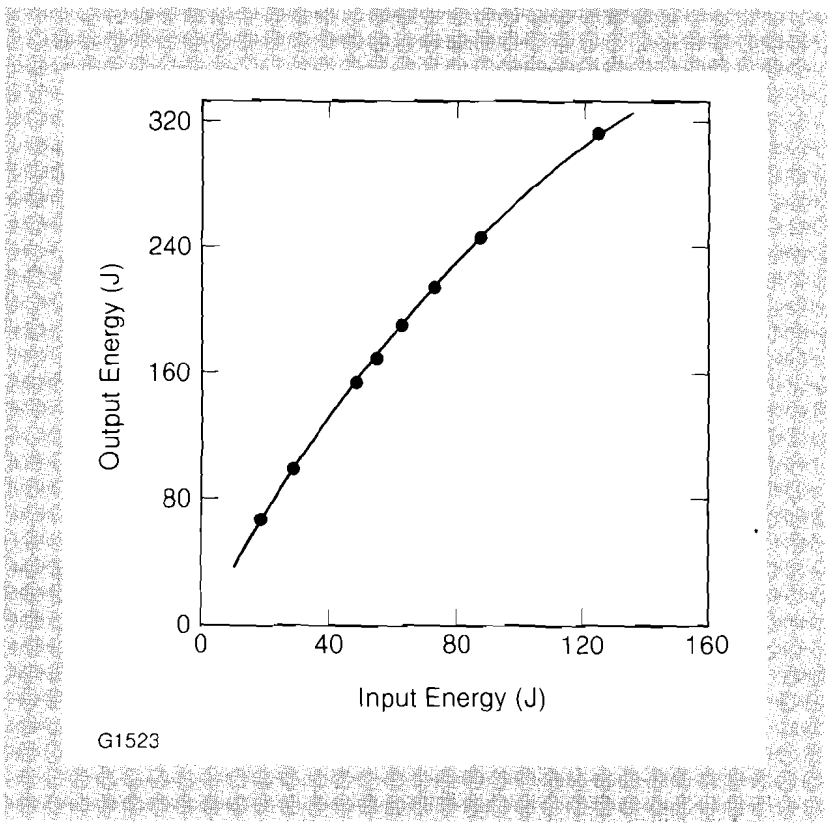

Fig. 21.3
One-nanosecond performance for a four-unit, single-passed active mirror booster to GDL. One of the four 2.5%-doped LHG-8 active mirrors was AR-coated on its front surface.

The near-field distribution, measured after the final spatial filter, indicates that the new amplification chain does not adversely affect the energy distribution. Preliminary phase measurements, using lateral shearing interferometry, have indicated that the collimating lens at the input to the active mirror sufficiently compensates the positive defocus that is inherent in slab amplifiers cooled through the rear surface.

Several experiments were conducted to evaluate beam alignment and focusing accuracy as well as beam focusability. X-ray pinhole photography has shown that the energy distribution has a triangular envelope for focusing conditions ahead of best focus. Equivalent-target-plane photography concurs but yields a more accurate picture of the energy

distribution within this envelope. The triangular shape originates from the cumulative wave front distortion introduced to each unit by the three-point mounting of the slab. Preliminary cw tests indicate that most of this distortion can be removed by properly adjusting the mounts after installation (see Fig. 21.4). Furthermore, rotation of two active mirror holders is expected to change this distribution into a less-pronounced hexagonal envelope. Although our effort to obtain uniform, round intensity distributions at the target plane continues, the beam envelope control inherent in the active mirror mounting design will be used to study alternate methods of intensity and phase correction. These are currently under investigation in the LLE uniformity program.

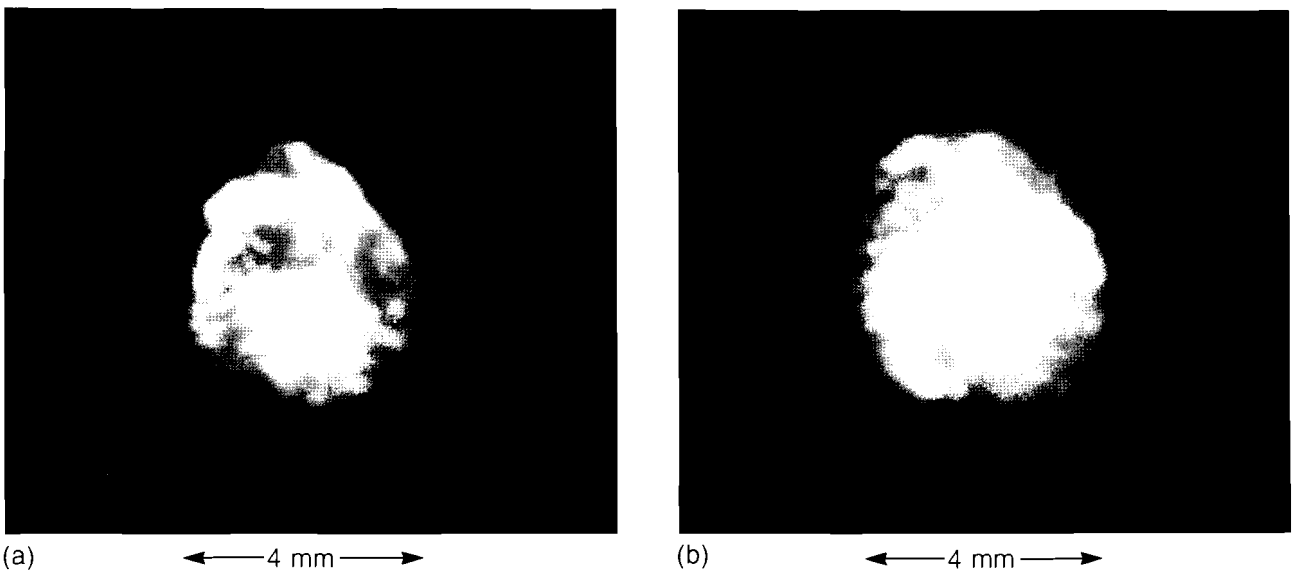

G1527

Fig. 21.4
A quasi-far-field intensity distribution from a YAG alignment laser in GDL shows the triangular envelope resulting from the cumulative wave-front deformation of four active mirrors (a). Active control of this distortion, obtained from proper adjustment of the mounts, is illustrated with the removal of most of the distortion (b).

In summary GDL has been upgraded with four 25-cm-diameter active mirror amplifiers to generate in excess of 300 J at 1054 nm in 1-ns pulses. Recent progress in hardware development involving a new active mirror mounting and sealing design has resulted in low slab distortion and increased reliability. Active mirror beam characterization has provided useful information that is the basis for further active mirror development. Concurrent with this upgrade, liquid crystal circular polarizers were tested and installed in the GDL amplifier chain.

ACKNOWLEDGMENT

This work was supported by the U.S. Department of Energy Office of Inertial Fusion under agreement number DE-FC08-85DP40200 and by the Laser Fusion Feasibility Project at the Laboratory for Laser Energetics which has the following sponsors: Empire State Electric Energy Research Corporation, General Electric Company, New York State Energy Research and Development Authority, Northeast Utilities Service Company, Ontario Hydro, Southern California Edison Company, The Standard Oil Company, and University of Rochester. Such support does not imply endorsement of the content by any of the above parties.

REFERENCES
1. J. Hoose and J. Soures, presented at the Conference on Laser Engineering and Applications, paper 4.1 (1975).
2. Laboratory for Laser Energetics Annual Report **1**, 10–18 (1977).
3. J. A. Abate, L. Lund, D. Brown, S. Jacobs, S. Refermat, J. Kelly, M. Gavin, J. Waldbillig, and O. Lewis, *Appl. Opt.* **20**, 351 (1981).
4. D. C. Brown, J. A. Abate, L. Lund, and J. Waldbillig, *Appl. Opt.* **20**, 1588 (1981).

1.D Retrofit of the GDL System with Liquid Crystal Polarizers

Brewster-angle linear polarizers composed of alternating high- and low-index, thin-film layers that have been deposited on glass substrates have been utilized in the GDL system at LLE since it was first constructed. Produced by standard e-gun deposition technology in apertures ranging from 2 cm to 20 cm, these optical elements routinely achieve polarization levels of 200 to 500:1 at 1054 nm with good laser damage resistance. They are essential to the operation of electro-optic switching devices such as Pockels cells. Three disadvantages to Brewster-angle polarizers include environmental instability, tendency to displace the laser system beamline, and physical space requirements.

We have recently replaced six Brewster-angle linear polarizers in GDL with liquid crystal (LC) polarizers, varying in clear aperture from 38 mm to 100 mm.[1] Figure 21.5 shows the locations of the liquid crystal cells

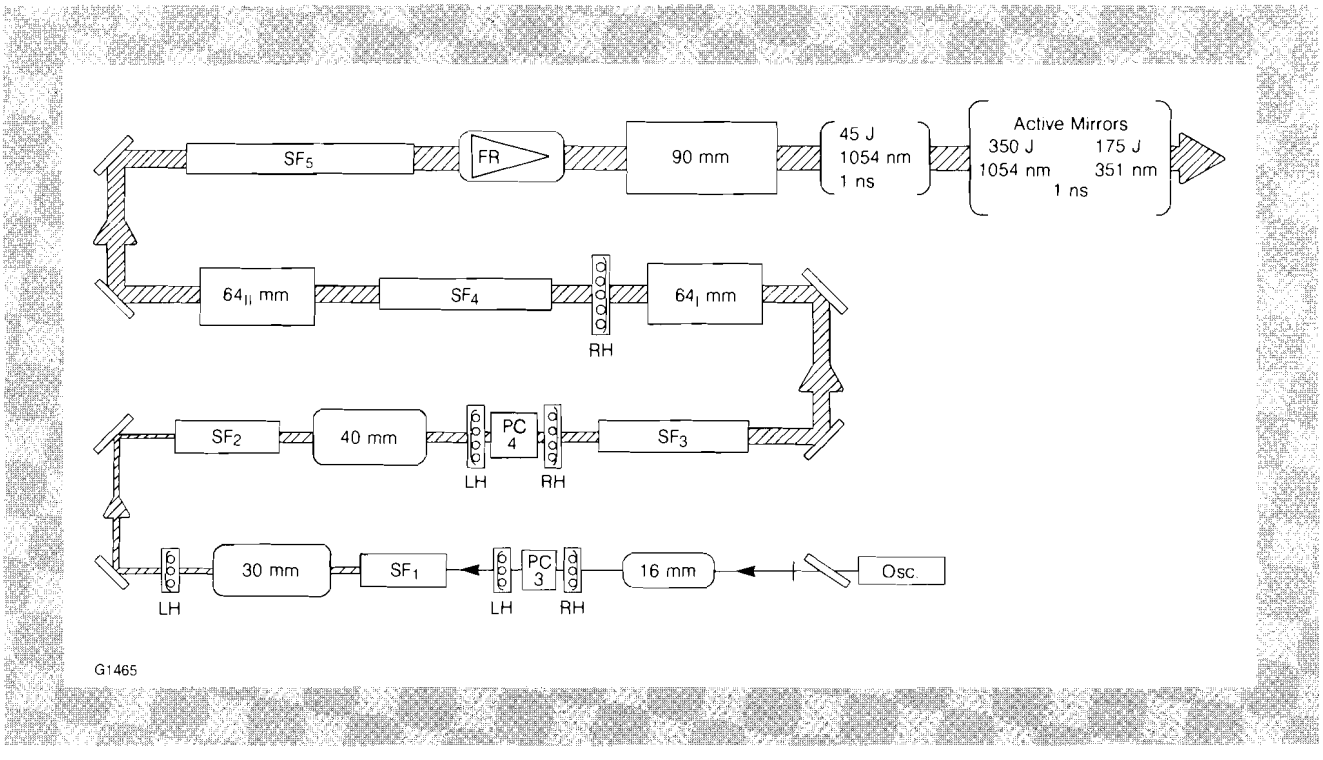

Fig. 21.5
GDL Nd:glass laser system with liquid crystal polarizers. The six circular polarizers vary in clear aperture from 38 mm to 100 mm and permit the propagation of circularly polarized laser radiation through most of the beamline.

in the system, which has been reconfigured to drive active mirror amplifiers. Liquid crystal polarizers have none of the disadvantages associated with Brewster-angle polarizers and offer additional features not available with any other polarizer technology. Figure 21.6 shows how, in addition to serving as polarization elements for electro-optic switches, liquid crystal cells can provide optical isolation or back reflection protection. This versatility has permitted us to incorporate the following changes in reconfiguring the GDL system:

1. propagation of circularly polarized laser radiation through the entire front end, minimizing stress birefringence induced by the laser rods;
2. relocation of the Faraday rotator toward the output end of the system, providing for better protection against system back reflection;
3. reduced concern with back reflected ghosts, due to the isolation properties of the LC polarizers;
4. improved throttle adjustment at the oscillator input to the beamline with the use of circular polarization; and
5. ease of installation and alignment.

In this article we describe the in-house design, fabrication, installation, and testing of liquid crystal polarizers on GDL.

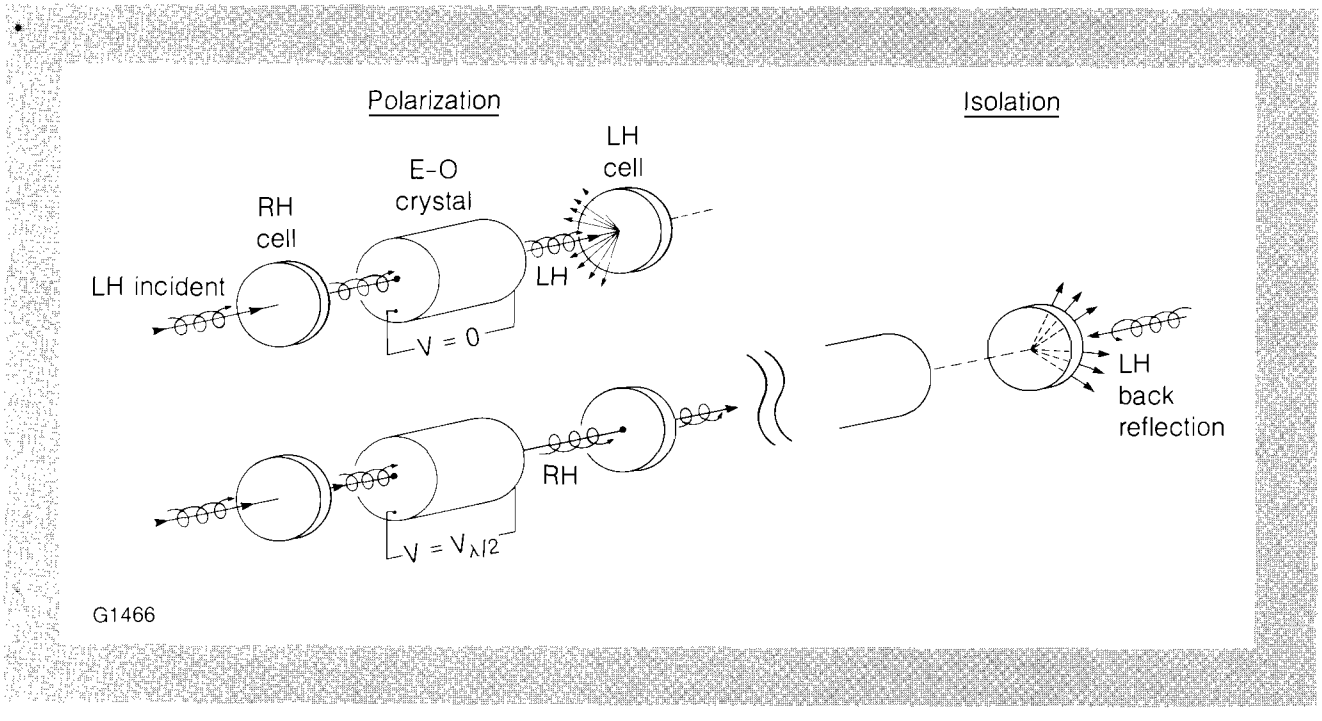

Fig. 21.6
Dual function of liquid crystal polarizers. Left-handed (LH) and right-handed (RH) circular polarizer elements may be fabricated and installed to perform traditional polarizer/analyzer functions in electro-optic switch-out devices. In addition, they act as optical isolators to prevent beamline component damage due to specular back reflections from fusion targets or ghosts.

The uses of liquid crystals for high-power laser applications have been discussed in the literature[2,3,4] and in previous volumes of LLE Review. In Volume 5 we described the property of selective reflection in cholesteric liquid crystal cells and the possibility of their use as optical isolators. Volume 6 contained research results for nematic liquid crystals as wave plates, and in Volume 15 we presented the concept of liquid

crystal, laser-blocking notch filters. Briefly reviewed, selective reflection occurs in organic liquid crystal compounds when left-handed (LH) or right-handed (RH) chiral additives are mixed into base nematics so that a helical twist structure results. As Fig. 21.7 shows, if the pitch P, characteristic of this twisted structure, satisfies the equation

$$\lambda_o = \bar{n}P \quad (1)$$

where $\bar{n}$ is the average refractive index of the liquid, then incident laser radiation at wavelength λ_o experiences Bragg-like interference and diffuse reflection for that circularly polarized component that rotates in the same sense as the helical structure. By using two cells in tandem, each filled with a fluid layer whose pitch and refractive index are tuned by compound blending to satisfy Eq. (1) but with *opposite* chirality, laser radiation of any arbitrary polarization state can be polarized and rejected by the cells. They act as a pair of crossed, circular polarizers at λ_o.

Fig. 21.7
Selective reflection and Bragg-like interference. The chiral structure of liquid crystals will selectively reflect incident laser radiation if the laser's sense of circular polarization and wavelength equal the product of helical pitch times average liquid refractive index. Otherwise, no interaction occurs.

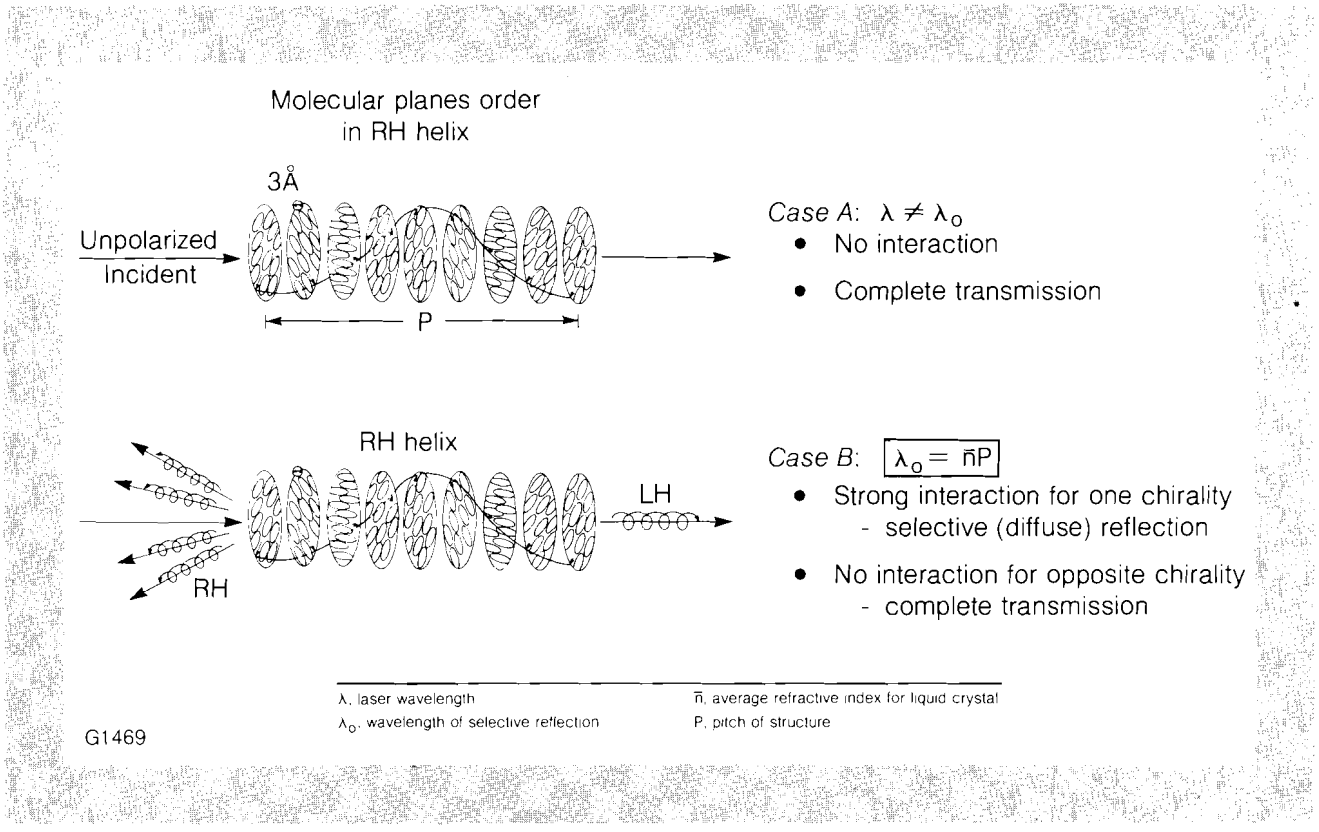

Figure 21.8 shows spectral absorptance in unpolarized light for LH and RH cells tuned to 1064 nm. Scanned separately, each fluid exhibits a selective reflection peak with few other features between 300 nm and 2000 nm. When scanned together, the composite exhibits strong extinction near 1064 nm.

Cell fabrication begins with selection of the compound. Table 21.I lists the pure, base nematics that we have selected from commercial sources. They represent eutectic mixtures of long, rodlike molecules whose terminal and bridging groups are chosen to optimize properties such as melting and clearing points, viscosity, birefringence, optical

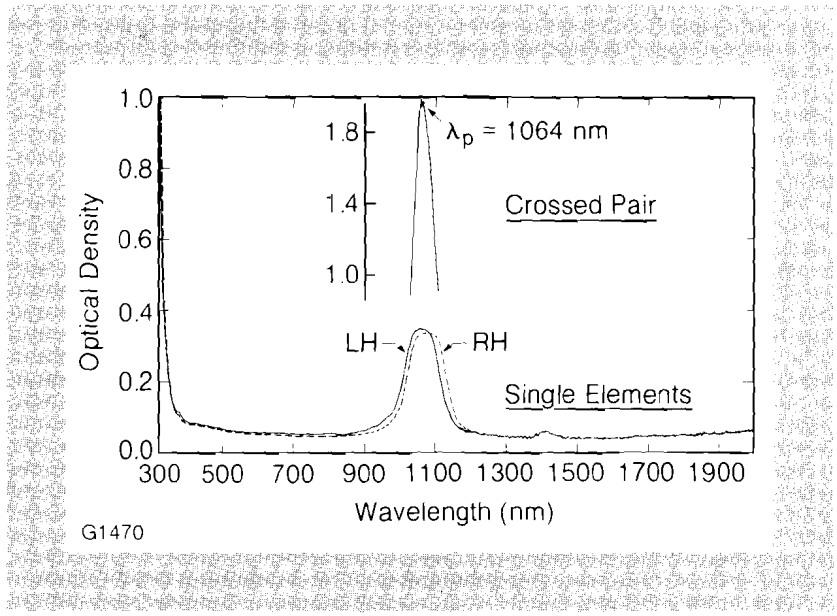

Fig. 21.8
Spectral transmission through liquid crystal polarizers. Single LH and RH element scans indicate that, apart from regions of increased optical density due to selective reflection, the spectral transmission of liquid crystal polarizers is featureless. Crossed polarizers exhibit blocking extinction at any desired wavelength, which is determined by tuning liquid crystal pitch with composition mixing.

transmittance, and environmental stability. The base nematics are all liquids at room temperature. The LH and RH chiral additives listed in Table 21.I may be solids (wax or powder) or liquids. The quantity of additive required for pitch tuning depends upon the intrinsic pitch of the substance (150 nm for CB15, 800 nm for C15), but it is usually of the order of 10–20 wt.%. Compound mixing is performed at elevated temperatures near 70°C to promote dissolution of the chiral additive.

Table 21.I
Base nematics and chiral additives.

Nematics

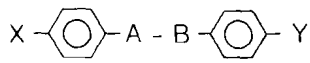

X, Y	A - B
Cyano-CN	Schiff-CH = N-
Alkyl-$CH_3(CH_2)_n$	Azoxy-N = N(O)-
Alkoxy-$CH_3(CH_2)_nO$	Ester-COO-

Merck: Licristal V, ZLI1646
BDH: E7, E8, ... E44
Roche: TN-403, TN701

LH Additives

COC, ZLI-811 } wax

C15, CN } powder

$CH_3(CH_2)_7COOC_{27}H_{45}$

RH Additives

CAA, S1082, CE1,2, . . . 7 } solid

CB15 fluid

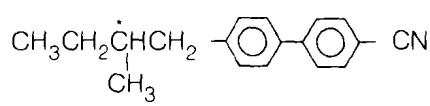

G1472

The recipe for circular polarizer fabrication is as follows:

(1) choose supporting substrate type (usually BK-7) and diameter (20–100 mm for present work);

(2) unidirectionally buff inner substrate surfaces with 1/10-μm diamond paste to create a preferred alignment direction and to provide wall anchoring for the liquid crystal molecules;

(3) heat substrates and tuned liquid crystal compound to ~70°C, apply 12-μm-thick Mylar spacer tabs, and form an air-gap sandwich;

(4) fill air-gap with heated fluid using capillary action;

(5) quench cell to room temperature and shear one substrate with respect to the other by 1/2 mm to orient the pitch structure along the beam propagation direction (see Fig. 21.9); and

(6) adjust cell for zero wedge in an interferometer and seal the fluid edge with epoxy.

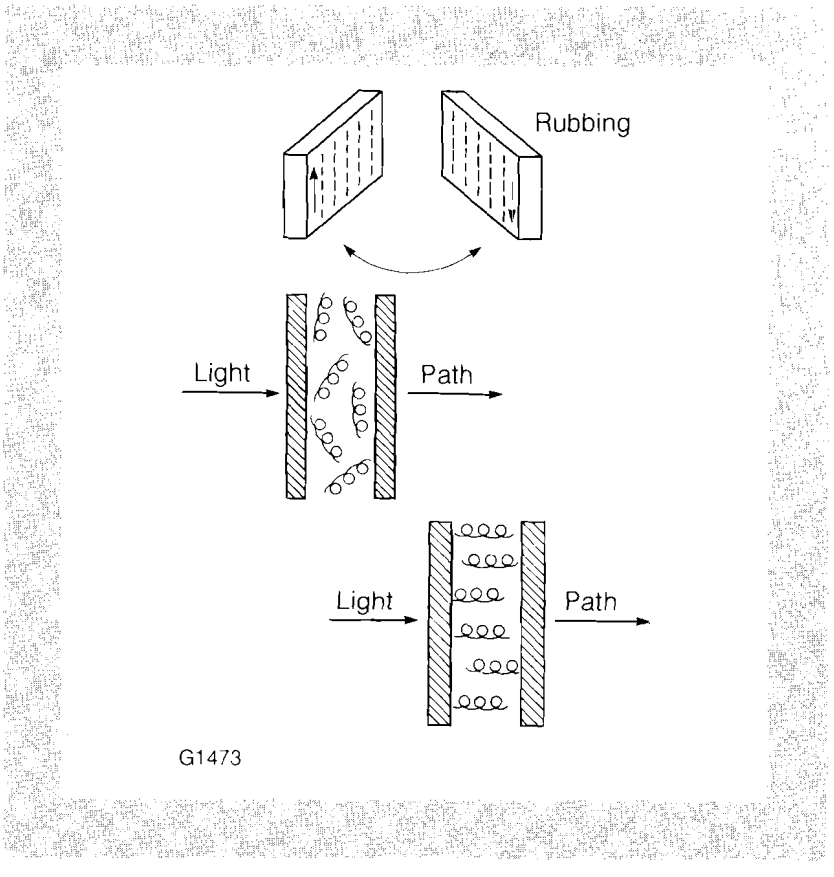

Fig. 21.9
Liquid crystal polarizer fabrication. Substrate inner surface rubbing helps to orient the rodlike liquid crystal molecules which contact the cell boundaries. A mechanical shear after the cell has been assembled tips molecular helices normal to the laser beam propagation direction, thereby minimizing scatter losses for the preserved polarization and maximizing extinction for the rejected polarization.

We have determined that fluid paths of 11–18 μm provide optimum polarization for the 1000-nm wavelength regime. The uniformity of fluid thickness across the polarizer clear aperture does not affect performance, as long as the layer exceeds a minimum of 10 pitch lengths. Transmission for the preserved polarization through a single element approaches 98%. Blocking extinction through crossed polarizers approaches 10^4.

The angular sensitivity of liquid crystal polarizers can be minimized by using base nematics whose birefringence Δn is large. Composition detuning to the long-wavelength side of the laser wavelength may also be employed to create polarizer elements whose angular performance resembles that shown in Fig. 21.10. Extinction from 0 to $\pm 20°$ off normal in excess of 10^3 has been demonstrated.

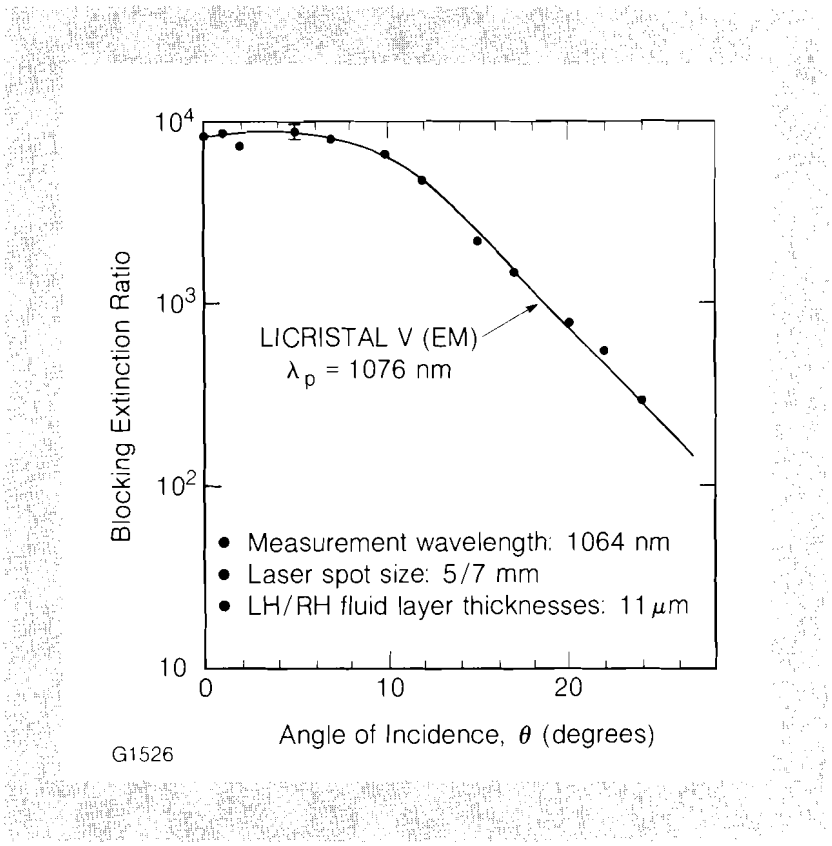

Fig. 21.10
Blocking extinction and angular sensitivity. Liquid fluid paths of between 11 and 18 μm are adequate to provide crossed polarizer blocking extinction levels of 10^4. The use of highly birefringent base nematics promotes selective reflection bandwidth in excess of 150 nm (FWHM). This in turn enables liquid crystal polarizers to be relatively insensitive to angle of incidence effects.

We have found that the temperature sensitivity of liquid crystal polarizers depends upon the type of base nematic and the type and quantity of chiral additive. Center-wavelength temperature shifts from 0.35 to 1.4 nm per °C have been measured. This level of sensitivity presents no problem to the use of these devices in our laboratory, where temperature is controlled to $\pm 3°C$.

A series of on-line laser damage tests was performed on 50- to 100-mm-diameter cells using the 1054-nm output of the GDL system. The RH combination of CB-15 in nematic E7 was found to be damage resistant to average fluences of 3 J/cm^2 (1 ns). LH polarizer cells failed at substantially lower fluences of less than 0.2 J/cm^2. Failure is determined by polariscopic observation of bubble growth in irradiated cells. We suspect that the primary reason for low damage thresholds in LH fluids is the lack of a room temperature, liquid chiral additive, or inadequate dissolution of the LH solid during fluid composition tuning. Our interim solution to this problem has been to employ RH element/half-wave-plate combinations to simulate the three LH elements indicated in Fig. 21.5.

A comparison of liquid crystal polarizers with other polarizer technologies is given in Table 21.II. Liquid crystals offer the advantages of high optical quality at large apertures, high contrast with angular insensitivity, high transmission for the preserved polarization, and environmental stability. They represent the only polarizer technology that, by itself, can provide back-reflection protection during standard use. Work is presently being conducted to understand and solve the LH-element, laser-damage problem.

Attribute	Crystal Prism	Brewster Thin Film	Dielectric Cube	Dyed Plastic	Liquid Crystal
• Optical quality at large apertures	no	yes	no	no	yes
• High contrast with angular insensitivity	no	no	no	yes	yes
• High transmission for passed polarization	yes	?	yes	no	yes
• Environmental stability	yes	no	yes	yes	yes
• Laser-damage resistance	some	yes	some	no	adequate
• Back-reflection protection	no	no	no	no	yes

G1479

Table 21.II
Comparison of polarizer technologies.

ACKNOWLEDGMENT

This work was supported by the U.S. Department of Energy Office of Inertial Fusion under agreement number DE-FC08-85DP40200 and by the Laser Fusion Feasibility Project at the Laboratory for Laser Energetics which has the following sponsors: Empire State Electric Energy Research Corporation, General Electric Company, New York State Energy Research and Development Authority, Northeast Utilities Service Company, Ontario Hydro, Southern California Edison Company, The Standard Oil Company, and University of Rochester. Such support does not imply endorsement of the content by any of the above parties.

REFERENCES

1. S. D. Jacobs, K. A. Cerqua, T. J. Kessler, W. Seka, and R. Bahr, "Retrofit of a High-Power Nd:Glass Laser System with Liquid Crystal Polarizers," 16th Annual Symposium on Optical Materials for High-Power Lasers, Boulder, CO, 15–17 October 1984.
2. S. D. Jacobs, "Liquid Crystals for Laser Applications," in *CRC Handbook Series of Laser Science and Technology*, Vol. III, edited by M. J. Weber (in press).
3. S. D. Jacobs, *SPIE Proceedings*, Vol. 307: *Polarizers and Applications*, San Diego, CA, (1981), pp. 98–105.
4. S. D. Jacobs, J. A. Abate, K. A. Bauer, R. P. Bossert, and J. M. Rinefierd, *Technical Digest – CLEOS/ICF'80*, San Diego, CA (1980), pp. 128–129.